



ELSEVIER

Available online at [www.sciencedirect.com](http://www.sciencedirect.com)

SCIENCE @ DIRECT®

Earth and Planetary Science Letters 214 (2003) 153–165

EPSL

[www.elsevier.com/locate/epsl](http://www.elsevier.com/locate/epsl)

# Azimuthal anisotropy and phase velocity beneath Iceland: implication for plume–ridge interaction

Aibing Li\*, Robert S. Detrick

*Department of Geology and Geophysics, Woods Hole Oceanographic Institution, 360 Woods Hole Road, Woods Hole, MA 02543, USA*

Received 7 March 2003; received in revised form 30 June 2003; accepted 7 July 2003

## Abstract

We have determined the pattern of azimuthal anisotropy beneath Iceland from shear-wave splitting and Rayleigh wave tomography using seismic data recorded during the ICEMELT and HOTSPOT experiments. The fast directions of shear-wave splitting are roughly N–S in western Iceland and NNW–SSE in eastern Iceland. In western Iceland azimuthal variations in Rayleigh wave phase velocity show that fast directions are close to the plate spreading direction at short periods of 25–40 s and roughly parallel to the Mid-Atlantic Ridge at longer periods of 50–67 s. Beneath the rift zones in central Iceland, we find a ridge-parallel fast direction at periods of 25–40 s and significantly weaker azimuthal anisotropy at periods of 50–67 s. The 2-D variation of isotropic phase velocity at periods of 33–67 s indicates that the lowest velocities are beneath the rift zones in central Iceland rather than above the plume conduit in southeast Iceland. While ridge-parallel alignment of melt films might contribute to anisotropy above 50 km depth beneath the rift zones, the overall observations are consistent with a model in which plume-influenced, hot, buoyant mantle rises beneath the Mid-Atlantic Ridge at depths greater than 50 km and is preferentially channeled along the ridge axis at the base of the lithosphere beneath Iceland. The shear-wave splitting results are attributed primarily to a N–S mantle flow at depths greater than 100 km.

© 2003 Elsevier B.V. All rights reserved.

*Keywords:* Iceland; azimuthal anisotropy; phase velocity; Rayleigh wave; tomography

## 1. Introduction

The Iceland hotspot is centered on the Mid-Atlantic Ridge (Fig. 1), making this region an ideal place for studying the interaction of a mantle plume with a mid-ocean ridge. A V-shaped pat-

tern of bathymetry and gravity anomalies along the Reykjanes Ridge south of Iceland, first recognized by Vogt [1], has been interpreted as the result of a pipe-like flow of mantle plume material along the Mid-Atlantic Ridge away from Iceland [2]. Geochemical evidence from variations of rare earth and trace element concentrations along the Reykjanes Ridge [3] also indicates that Iceland plume material has been transported several hundreds of kilometers southward along the Mid-Atlantic Ridge. Numerical and laboratory experiments in plume ridge systems have demonstrated

\* Corresponding author. Present address: University of Houston, Department of Geosciences, Houston, TX 77204, USA. Tel.: +1-713-743-9313; Fax: +1-713-748-7906.

E-mail address: [ali2@mail.uh.edu](mailto:ali2@mail.uh.edu) (A. Li).

that the width of plume material along a ridge axis is controlled by the volume of plume flux, spreading rate of the plates, and other parameters [4,5]. The most common models of plume–ridge interaction in Iceland include radial flow, where buoyant plume material spreads laterally from the plume center in a pancake-like fashion at the base of the rigid lithosphere [6–8], and focused flow where plume material is preferentially channeled to and along the axis of the nearby spreading center [9]. Both models can produce the V-shaped bathymetric and gravity patterns observed along the Reykjanes Ridge.

Two broadband seismic experiments, ICEMELT [10] and HOTSPOT [11] (Fig. 1), deployed in Iceland from 1995 to 1998 provide data that can be used to investigate plume–ridge interaction beneath Iceland. P and S body wave tomographic models in Iceland have revealed a relatively narrow (< 200 km), low-velocity conduit at depths of ~100–400 km beneath Iceland which has been associated with the Iceland plume [12–14]. Using P to S converted phases in receiver function analysis, Shen et al. [15] imaged a relatively thin transition zone beneath Iceland and argued for a low-

er mantle origin of the Iceland plume. However, the structure in the uppermost mantle (< 100 km) beneath Iceland, where a plume head is expected, is not well resolved in body wave inversions.

Seismic anisotropy in the upper mantle is generally believed to be largely caused by strain-induced, lattice-preferred orientation of olivine *a*-axes. The fast direction of seismic anisotropy is consequently interpreted as a direct indication of flow direction in the upper mantle [16]. The complex tectonics of Iceland suggests that mantle flow beneath Iceland must be complicated as well. Possible flow components include flow related to plate spreading, channeling flow along the ridge, radial flow away from the plume center, and flow associated with the absolute plate movement [17] (Fig. 2). Menke et al. [18] observed ridge-parallel anisotropy in the crust in southwest Iceland. Gaherty [19] analyzed the difference between  $V_{SV}$  and  $V_{SH}$  derived from Rayleigh and Love wave dispersion along the Reykjanes Ridge to infer buoyant upwelling beneath this part of the Mid-Atlantic Ridge. Azimuthal anisotropy from surface wave tomography on a global scale [20] shows complex, frequency-dependent anisotropy in the North Atlantic, but does not have sufficient lateral resolution to determine anisotropy beneath Iceland. Bjarnason et al. [21] measured shear-wave splitting at the ICEMELT stations and explained their observations by shear between absolute plate motion and a return mantle flow beneath Iceland.

In this study upper mantle anisotropy beneath Iceland has been determined from shear-wave splitting and Rayleigh wave phase velocities using data recorded in the ICEMELT and HOTSPOT experiments. These two approaches are complementary: splitting measurements of anisotropy have relatively high lateral resolution if station coverage is dense but poor vertical resolution, while Rayleigh waves can resolve variations in anisotropy with depth, but have poorer lateral resolution. We have solved for Rayleigh wave phase velocities at periods of 25–67 s, which are most sensitive to velocity variations in crust and uppermost mantle where current body wave tomography models have little resolution. We use these results to show that plume material beneath

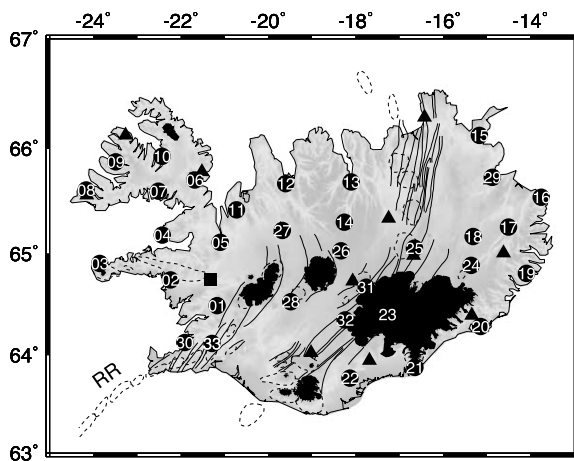


Fig. 1. Locations of broadband seismic stations in Iceland. Triangles are stations of the ICEMELT experiment [10], black dots with station numbers inside are stations of the HOTSPOT experiment [11], and the square is station BORG, a GSN station. Thin black lines indicate fissure swarms and rift zones in Iceland. Central volcanoes are marked by dashed curves. RR stands for the Reykjanes Ridge. White-shaded areas are icecaps.

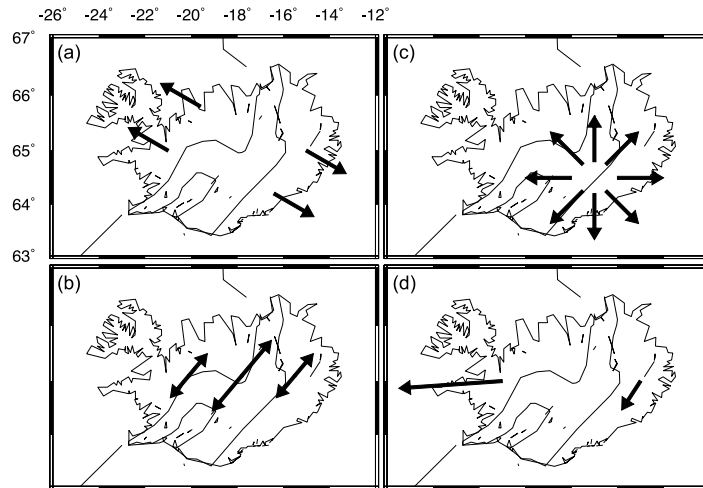


Fig. 2. Cartoon showing possible mantle flow components beneath Iceland. (a) Mantle flow in plate spreading direction. (b) Flow channeled along the Mid-Atlantic Ridge. (c) Radial flow away from the plume center. (d) Flow related to absolute plate movement. Flow directions are schematic except the absolute plate motions in d, which are obtained from NUVEL-1 [17].

Iceland appears to be preferentially channeled along the Mid-Atlantic Ridge at the base of the lithosphere.

## 2. Anisotropy from shear-wave splitting

We measured fast polarization directions and delay times of shear-wave splitting using SKS, PKS, SKKS, and PKKS phases recorded at 33 HOTSPOT stations and one Global Seismic Network (GSN) station (Fig. 1). In order to have clear core reflected phases, events with  $M_b > 6.0$  and epicentral distances from  $85^\circ$  to  $150^\circ$  were selected. We first tried the standard method of Silver and Chan [22] to obtain individual splitting measurements. However, most of these measurements are not well constrained, probably due to high attenuation beneath Iceland that reduces signal/noise ratios on seismograms. We consequently used the method of Wolfe and Silver [23] that allows several events at one station to be stacked and yields an average result for each station.

Our anisotropy measurements are shown in Fig. 3 and also listed in Table 1. Fast directions are N–S to NNE–SSW in western Iceland (west of  $21^\circ\text{W}$ ) and generally NNW–SSE in eastern Iceland (east of  $16^\circ\text{W}$ ). Many stations in central Ice-

land along the rift zones do not have high-quality shear-wave splitting data, which might be due to high attenuation beneath the spreading axis. Anisotropy beneath the rift zones in central Iceland is relatively complex compared to that in western and eastern Iceland. These results differ from

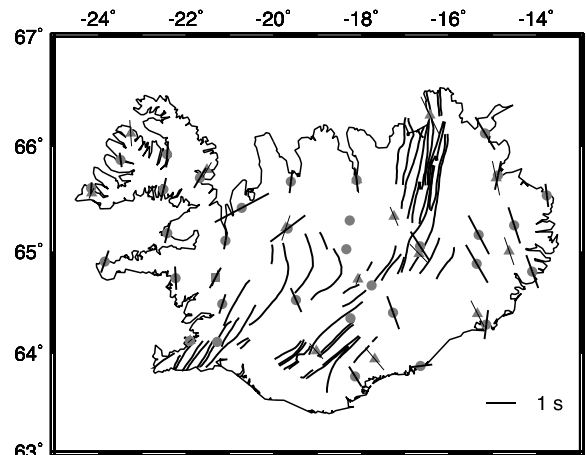


Fig. 3. Shear-wave splitting results at the HOTSPOT stations (gray triangles) from this study and at the ICEMELT stations (gray circles) obtained by Bjarnason et al. [21]. Azimuthal anisotropy is shown as black bars at each station. The strike of a bar indicates fast polarization direction and the length is proportional to the magnitude of delay time.

those in the MELT area at the East Pacific Rise [24], where the fast direction of azimuthal anisotropy is perpendicular to the ridge axis and parallel to the direction of plate spreading. The observed fast directions in Iceland from shear-wave splitting measurements are not consistent with any expected simple mantle flow models, such as WNW–ESE flow associated with the plate spreading, ridge-parallel flow, radial flow from the plume center, or shear due to absolute plate motions (Fig. 2).

The NNE and NNW fast directions we observe in Iceland are consistent with regional-scale anisotropy in the North Atlantic constrained from S and SS phases by Yang and Fischer [25], suggesting that mantle anisotropy in Iceland might be significantly affected by large-scale flow, such as mantle return flow in the North Atlantic [26]. Our

splitting observations at the HOTSPOT stations agree very well with those at the ICEMELT stations obtained by Bjarnason et al. [21] (Fig. 3). They hypothesized that the observed anisotropy indicated shear between absolute plate motions and a larger-scale, deeper mantle return flow in a NNW direction. If this interpretation is correct, mantle anisotropy beneath Iceland is not strongly influenced by the Iceland plume or Mid-Atlantic Ridge spreading. However, because shear-wave splitting integrates the effects of anisotropy from the core–mantle boundary to the Earth’s surface, these results do not necessarily mean that mantle flow associated with the Iceland plume and ridge-spreading does not exist, but indicate its net contribution to shear-wave splitting is small. This can occur, for example, if plume–ridge flow is complicated or confined in a relatively thin layer.

Table 1  
Shear-wave splitting results at the HOTSPOT stations

Station	Latitude	Longitude	$\phi$ (°)	$\delta t$ (s)	Number of phases
HOT01	64.4941	−21.1679	18 ± 6	0.7 ± 0.03	5
HOT02	64.7459	−22.2323	−3 ± 3	0.8 ± 0.05	12
HOT03	64.9073	−23.8523	19 ± 9	0.8 ± 0.1	3
HOT04	65.1805	−22.4233	14 ± 6	0.7 ± 0.05	5
HOT05	65.1097	−21.0964	10 ± 13	0.6 ± 0.1	6
HOT06	65.7050	−21.6778	31 ± 2	0.8 ± 0.03	13
HOT07	65.5984	−22.5100	13 ± 3	0.8 ± 0.07	4
HOT08	65.6099	−24.1614	4 ± 3	0.4 ± 0.03	7
HOT09	65.8739	−23.4866	−8 ± 4	0.5 ± 0.05	7
HOT10	65.9268	−22.4284	4 ± 2	0.9 ± 0.05	12
HOT11	65.4222	−20.7218	62 ± 2	2.1 ± 0.38	3
HOT12	65.6707	−19.5996	7 ± 10	0.8 ± 0.12	3
HOT13	65.6859	−18.0998	−6 ± 5	0.8 ± 0.08	4
HOT15	66.1214	−15.1691	−31 ± 4	1.3 ± 0.08	2
HOT16	65.5408	−13.7535	−7 ± 6	0.8 ± 0.15	5
HOT17	65.2562	−14.5018	−22 ± 2	1.4 ± 0.05	9
HOT18	65.1659	−15.3087	−28 ± 2	1.5 ± 0.07	4
HOT19	64.8104	−14.0906	−20 ± 1	1.2 ± 0.12	5
HOT20	64.2878	−15.1392	7 ± 2	1.0 ± 0.03	9
HOT21	63.8765	−16.6410	83 ± 2	0.8 ± 0.07	3
HOT22	63.7698	−18.1306	−32 ± 3	0.8 ± 0.05	3
HOT23	64.4068	−17.2665	−30 ± 2	1.2 ± 0.12	4
HOT24	64.8862	−15.3535	−30 ± 2	1.5 ± 0.1	8
HOT25	65.0544	−16.6502	−33 ± 2	1.2 ± 0.05	4
HOT27	65.2254	−19.6736	53 ± 1	1.5 ± 0.18	10
HOT28	64.5325	−19.4842	−24 ± 3	0.9 ± 0.08	5
HOT29	65.7286	−14.8736	12 ± 9	1.0 ± 0.17	3
BORG	64.7474	−21.3268	29 ± 4	0.8 ± 0.05	7

### 3. Rayleigh wave phase velocity and azimuthal anisotropy

#### 3.1. Methodology

In order to provide additional constraints on velocity and anisotropy in the uppermost mantle beneath Iceland we have analyzed Rayleigh waves recorded at the ICEMELT and HOTSPOT stations. Rayleigh waves at different periods sample velocity structure at different depth ranges with the peak sensitivity at  $\sim 1/3$  of the wavelength. Rayleigh waves therefore have great potential to constrain the distribution of anisotropy with depth. In slightly anisotropic medium, Rayleigh wave phase velocity can be represented as  $c(\omega, \phi) = A_0(\omega) + A_1(\omega)\cos 2\phi + A_2(\omega)\sin 2\phi + A_3(\omega)\cos 4\phi + A_4(\omega)\sin 4\phi$ , where  $\omega$  is the frequency,  $\phi$  is the propagation direction of the wave,  $A_0$  is isotropic velocity coefficient, and  $A_1$ – $A_4$  are azimuthal anisotropic coefficients [27]. We ignored the  $4\phi$  terms in this study because the coefficients of  $A_3$  and  $A_4$  are small for Rayleigh waves. The amplitude of anisotropy is expressed as  $(A_1^2 + A_2^2)^{1/2}$ , and the fast propagation direction is represented as  $1/2 \arctan(A_2/A_1)$ .

Data from  $\sim 80$  teleseismic events recorded at

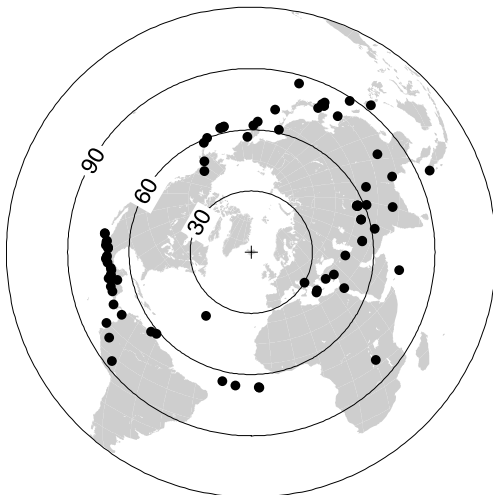


Fig. 4. Epicenters of earthquakes (black dots) used as sources in the ICEMELT and HOTSPOT experiments for Rayleigh wave tomography. The plot is centered on Iceland (the cross) using an azimuthal equidistant projection.

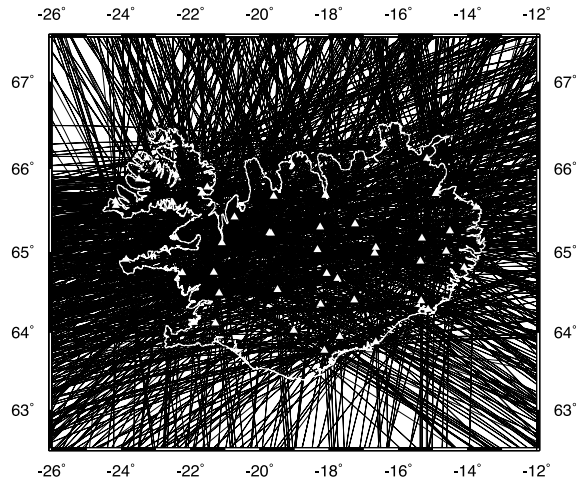


Fig. 5. Great circle ray paths to the ICEMELT and HOTSPOT stations (white triangles) at a period of 50 s. The coverage of ray paths varies with periods, but crossing ray paths are generally dense within Iceland.

the HOTSPOT and ICEMELT stations were used in this study (Fig. 4). The distribution of events shows good azimuthal coverage, which is a basic requirement for constraining anisotropy. The large number of stations and events ensures dense crossing ray paths in Iceland and its vicinity (Fig. 5), where high model resolution is expected. Fundamental mode Rayleigh waves at different periods were obtained by applying 10 mHz wide, fourth order, double-pass Butterworth filters to the vertical component seismograms at different center frequencies. Only clean Rayleigh wave trains that are consistent from station to station were kept in the data set.

We have applied a two plane wave inversion technique [28,29] in calculating phase velocities using both amplitude and phase data of Rayleigh waves. The essential feature of this method is the ability to account for non-plane wave energy in the incoming wavefield due to scattering or multipathing along ray paths, which are represented by two plane waves with unknown amplitude, phase, and propagation direction. We parameterized phase velocity in the study area by a grid (Fig. 6) that has relatively dense nodes in the center. The two plane wave parameters and phase velocities are solved simultaneously in the inversion. 2-D isotropic phase velocities can be obtained

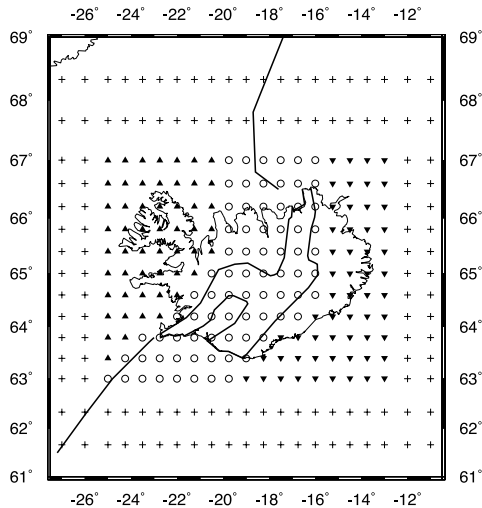


Fig. 6. Grid nodes used in Rayleigh wave inversions. In anisotropic inversions, black triangles, open circles, and inverse black triangles are grouped as western Iceland, central Iceland rift zones, and eastern Iceland, respectively.

by inverting for coefficient  $A_0$  at each node of the grid.  $A_1$  and  $A_2$  have to be inverted along with  $A_0$  in order to solve for azimuthal anisotropy. Ideally, 2-D variation of anisotropy can be obtained on the scale of a grid cell. However, in this case the number of model parameters for phase velocity and anisotropy is three times that for isotropic phase velocity alone, and they cannot be well resolved. To reduce the number of model parameters, and to account for lateral variations of azimuthal anisotropy, we assume that anisotropy is constant in three sub-regions and variable between them (Fig. 6) while isotropic phase velocities are allowed to vary by grid node. Since mantle anisotropy reflects deformation of the lithosphere and flow in the asthenosphere and is likely strongly associated with current and historical tectonics, we construct the three sub-regions according to major tectonic provinces in Iceland. They are western Iceland on the North American plate, eastern Iceland on the Euro-Asian plate, and Icelandic rift zones on the Mid-Atlantic Ridge. Any variation of anisotropy within each province will be averaged by this parameterization. However, the lateral variation of anisotropy within each sub-region may not be significant, as shear-wave splitting has shown that

anisotropy is relatively uniform in western Iceland and eastern Iceland, respectively.

### 3.2. Observations

We initially solved for average phase velocities in the study area by keeping  $A_0$  constant at all grid nodes in the inversion. In this case, there is only one model parameter for phase velocity at a given frequency. These velocities can be well resolved and their standard deviation is about 0.006 km/s. The average phase velocities beneath Iceland range from 3.63 km/s to 3.74 km/s at periods of 25–67 s (Fig. 7), which primarily sample velocity structure at depths of 20–100 km. The low phase velocities at periods of 25 s and 30 s indicate the presence of thick crust beneath Iceland. At periods greater than 30 s, the phase velocities are generally  $\sim 0.5$  km/s lower than those beneath the Pacific seafloor at ages of 0–4 Ma [30] and compatible with those beneath the youngest seafloor (0–0.8 Ma) at the East Pacific Rise [28], suggesting that the uppermost mantle of Iceland is hotter and/or more melt-rich than beneath a typical ocean spreading center. These very low mantle velocities beneath Iceland are presumably associated with the Iceland plume.

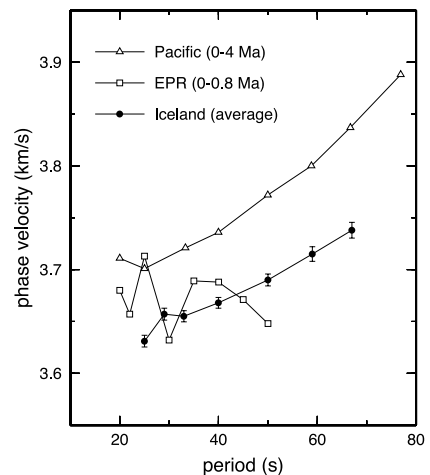


Fig. 7. Comparison of average phase velocities in Iceland (filled circles) from this study with those beneath young Pacific seafloor (open triangles) [30] and beneath the East Pacific Rise at ages of 0–0.8 Ma (open squares) [28].

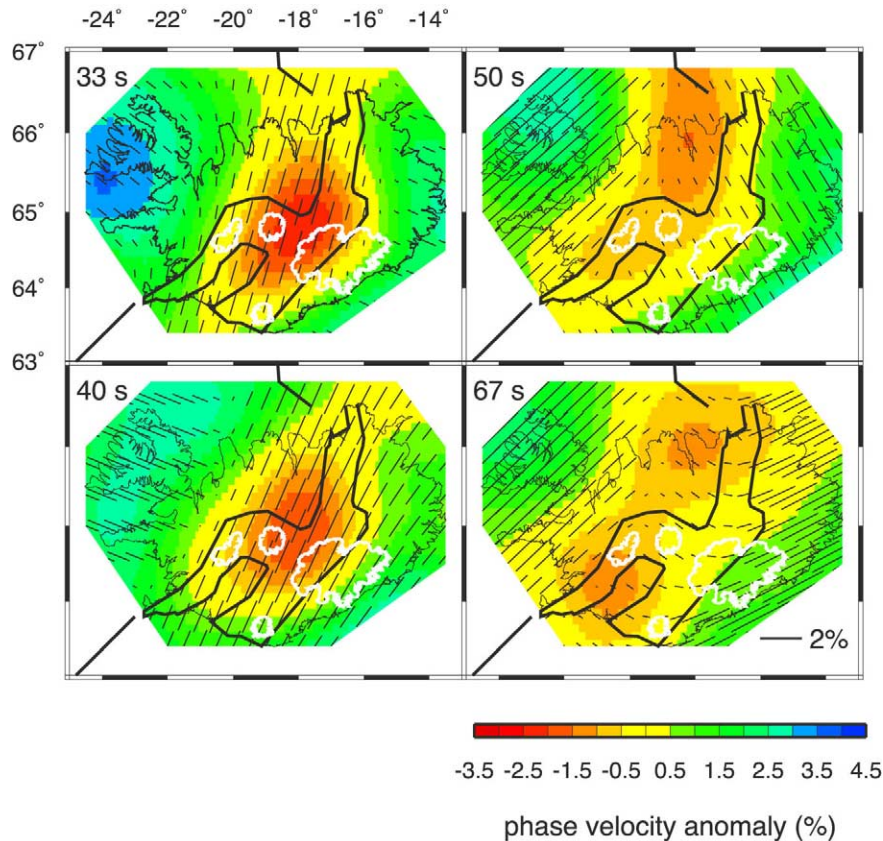


Fig. 8. Maps of phase velocity and azimuthal anisotropy at four periods (33, 40, 50, and 67 s). Color contours are isotropic phase velocity perturbations relative to the average values in Iceland shown in Fig. 7. Black bars indicate anisotropy in a map view. Strike of bars represents orientation of fast directions and bar lengths are proportional to the magnitude of anisotropy. A smoothing length of 80 km is used in generating these maps and maps shown in Fig. 10. Thick black lines mark the Mid-Atlantic Ridge rift zones. White lines are for icecaps.

Inversions for lateral variations of phase velocity were performed with minimum length and smoothing criteria. The average phase velocity at each period was used as the starting model and a smoothing length of 80 km was used in the inversion. Velocity anomaly maps at periods of 33, 40, 50, and 67 s are shown in Fig. 8. At periods of 33 and 40 s, the slowest anomaly is concentrated in central Iceland in a circular area. At periods of 50 and 67 s, the lowest phase velocities are found beneath the Icelandic rift zones rather than directly beneath the hotspot in southeastern Iceland. Higher velocities are imaged in western and eastern Iceland at these periods.

Azimuthal anisotropy obtained from Rayleigh waves is frequency-dependent and varies laterally

across Iceland. In the Icelandic rift zones, anisotropy is roughly constant at periods of 25–40 s with amplitudes of 1.5–2.0% and a fast direction of NNE–SSW, close to the strike of the ridge axis, while anisotropy is significantly weaker at periods of 50–67 s (Figs. 8 and 9b). In western Iceland, fast directions at periods of 25–40 s are generally oriented WNW–ESE, the plate spreading direction. The more consistent observation is the NE–SW fast directions from period 50 s to 67 s, which are parallel to the strike of the ridge (Figs. 8 and 9a). The fast directions in eastern Iceland seem to vary randomly at different periods (Figs. 8 and 9c), which cannot be caused by a realistic earth structure. This random variation of anisotropy is likely due to the large errors in measurements. As

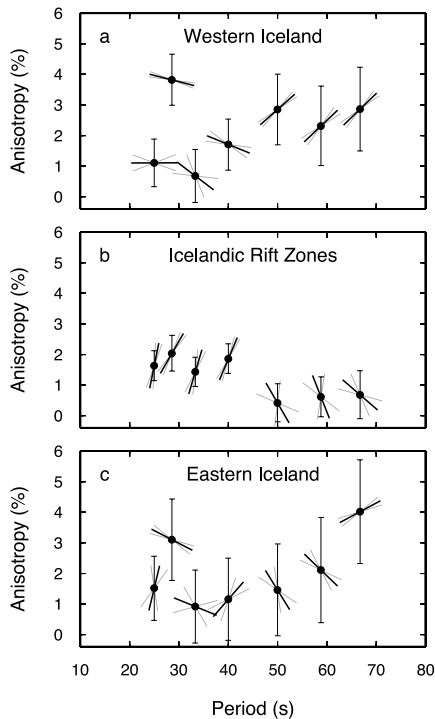


Fig. 9. Variations of azimuthal anisotropy with period in western Iceland (a), the Icelandic rift zones (b), and eastern Iceland (c). The strike of the thick black bars indicates fast directions of anisotropy in a map view with north corresponding to a positive  $y$ -axis. Thin black bars with caps represent one standard errors of anisotropy magnitude. Gray bars give one standard deviations for fast direction orientation.

shown in Fig. 9c, anisotropy in eastern Iceland is poorly constrained.

### 3.3. Model resolution

Model resolution is affected by the density of ray paths, the wavelength of Rayleigh waves, and the smoothing length used in the inversions. For a given frequency, resolution is higher in central Iceland than in western and eastern Iceland because crossing ray paths are denser within the station array than at its edges (Fig. 5). Thus phase velocity in central Iceland and anisotropy in the Icelandic rift zones are better resolved than elsewhere in Iceland. Model resolution decreases as Rayleigh wave wavelength increases. This is not only because there is an intrinsic limitation of

long-wavelength data for resolving small-scale heterogeneity, but also because the same error in phase corresponds to a larger error in travel time at a longer period. From this perspective, resolution of phase velocity and anisotropy at 67 s is poorer than at other periods in Fig. 8. The effect of smoothing length on resolution is not a factor in this study because we use the same length, 80 km, at all periods.

In order to estimate how well the important features observed in phase velocity and anisotropy (Fig. 8) are resolved, we conducted a series of resolution tests using synthetic data sets. Input models were constructed to reflect the main patterns in the observations, for instance, a circular-shaped low-velocity region in central Iceland at periods of 33 and 40 s and a ridge-centered, low-velocity band at 50 and 67 s. Anisotropy was assumed to be 1.5% with fast direction in N20°E and confined in the rift zones in central Iceland at short periods ( $< 40$  s) and in western Iceland at longer periods (Fig. 10). Synthetic data at periods of 33, 40, 50, and 67 s were generated from these models using the same ray paths as in the real data.

We first applied the two plane wave inversion technique to noise-free synthetic data sets and found that the input models can be almost perfectly recovered to periods of 50 s. At period of 67 s, artificial anisotropy starts to appear in eastern Iceland. Gaussian-distributed random noise was added to synthetic phases and amplitudes based on the noise level in the real data. Inversion results obtained using noisy synthetic data are shown in Fig. 10 for periods of 33 and 50 s. The low-velocity band along the rift zones and the circular-shaped low-velocity anomaly in central Iceland are largely recovered although the amplitude of the anomalies changes up to one contour level, 0.5%. In the rift zones, both fast direction and amplitude of anisotropy at 33 s and zero anisotropy at 50 s are well recovered. In western Iceland the direction of anisotropy is well resolved at 50 s while its amplitude is about 0.5% greater than in the input value. Artificial anisotropy is imaged in eastern Iceland at all periods and more pronounced with increasing period. Synthetic tests were also conducted for peri-

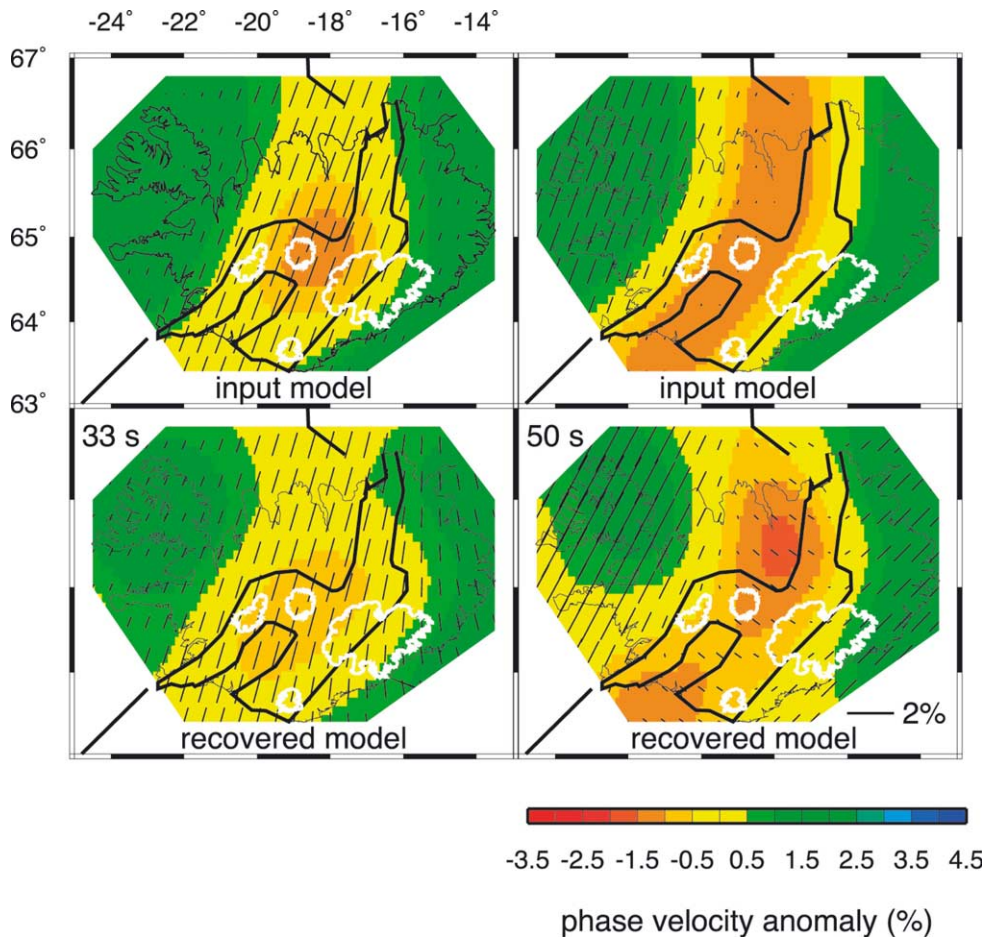


Fig. 10. Input and recovered models at 33 s (left) and 50 s (right). Color contours are phase velocity anomalies and black bars indicate azimuthal anisotropy as in Fig. 8.

ods of 40 s and 67 s and their solutions are similar to those at 33 s and 50 s respectively, except that the amount of artificial anisotropy is greater.

This artificial anisotropy arises partially from a trade-off between lateral variations in phase velocity and anisotropy. Fast directions in the rift zones would be NNW, perpendicular to the NNE-oriented low-velocity band, if anisotropy were purely caused by trade-off with velocity heterogeneity. The observed anisotropy in the rift zones shows NNE fast directions at short periods and close to zero anisotropy at longer periods which cannot be attributed to a trade-off with lateral variations in phase velocity. Anisotropy

in one sub-region can also be affected by a trade-off with anisotropy in a neighboring sub-region. This type of trade-off might exist between western Iceland sub-region and the rift zone sub-region where close to orthogonal fast directions are observed (Figs. 8 and 9). However, in the recovered models at periods of 33 s and 50 s (Fig. 10), artificial anisotropy in both regions is only about 0.5%, much less than the observed  $\sim 2\%$  anisotropy. While both types of trade-offs increase with increasing periods. At periods of less than 67 s, synthetic tests demonstrate that the effects of these trade-offs on anisotropy in Iceland are not significant.

## 4. Discussion

### 4.1. Phase velocity constraints on Iceland plume head

Rayleigh waves from 33 to 67 s primarily sample structure in the uppermost mantle from 40 to 100 km depth where the Iceland plume head is expected. The anomalously low average phase velocities beneath Iceland, compared to the East Pacific Rise (Fig. 7), indicate the presence of thicker crust and a hotter, more melt-rich mantle presumably associated with the Iceland plume. The 2-D phase velocity anomalies (Fig. 8) are calculated relative to these low average velocities and thus show lateral variations of velocity structure in a relative sense. The pattern of negative anomalies shown in Fig. 8, therefore, is not a direct reflection of the plume head. It is quite possible that the Iceland plume head spreads beneath the whole of Iceland, or over an even larger area [14].

The phase velocity maps at periods of 33 and 40 s show a negative, circular-shaped anomaly in central Iceland (Fig. 8a,b). This anomaly roughly corresponds to the thickest crust in central and southeastern Iceland [31,32] and agrees with the low-velocity region in the lower crust of central Iceland imaged by Allen et al. [31]. Anomalous phase velocities at 50 and 67 s (Fig. 8c,d) show a band of low velocities that approximately follow the trend of the rift zones in central Iceland that mark the location of the Mid-Atlantic Ridge. This ridge-centered negative anomaly might be caused by the accumulation of melt and/or hot plume material.

We do not observe an obvious expression of the plume conduit beneath southeastern Iceland that has been imaged in body wave tomography [12–14]. This is because our observations are more sensitive to structure above 100 km depth while body wave tomography mainly constrains structure below 100 km. Although the pattern of low phase velocities in Fig. 8 may reflect variations in temperature and/or the distribution of melt, lateral variations of isotropic phase velocity alone cannot distinguish between the different flow models shown in Fig. 2. However, mantle flow beneath Iceland can be constrained from anisotropy observations.

### 4.2. Anisotropy constraints on deep asthenospheric mantle flow

Because of the different vertical and horizontal resolution of azimuthal anisotropy determined from shear-wave splitting and Rayleigh waves, anisotropy measured using these two methods will disagree if anisotropy is not uniformly distributed laterally and/or with depth. Here we compare anisotropy obtained from shear-wave splitting and Rayleigh wave inversions in western Iceland where measurements from both methods are reliable. Rayleigh waves show evidence of two layers of anisotropy with a flow direction in a fossil plate spreading direction (WNW–ESE) at depths above  $\sim 50$  km and a ridge-parallel direction (NE–SW) to  $\sim 100$  km depth. In contrast, the shear-wave splitting results show a fast direction close to N–S. Because anisotropy constrained from Rayleigh waves varies in two layers above 100 km, its net effect on shear wave splitting is relatively small. We suggest that a deep asthenospheric flow in a roughly N–S direction at depths greater than 100 km is the primary cause of the shear-wave splitting anomalies observed in western Iceland. This type of deep mantle flow has also been suggested by Shen et al. [33] based on a tilting of the Iceland plume conduit, is required to explain the shear-wave splitting results at the stations of the ICEMELT experiment [21], and has been simulated in kinematic modeling of large-scale mantle flow governed by plate motions [26]. Better constraints on this large-scale asthenospheric mantle flow may come from anisotropy measured at stations far away from hotspot tracks and the Mid-Atlantic Ridge, where mantle flow is presumably much simpler than beneath Iceland.

### 4.3. Anisotropy evidence of buoyant flow

The weak azimuthal anisotropy observed at periods of 50–67 s beneath the central Iceland rift zones (Figs. 8 and 9a) may indicate the mantle is isotropic at the corresponding depth range of 50–100 km or that olivine  $a$ -axes are aligned nearly vertically. These interpretations correspond to passive upwelling and buoyant upwelling, respectively [34]. Anisotropy alone cannot distinguish

these two interpretations. If passive, plate-driven mantle flow exists under the spreading centers in Iceland, we would expect the fast direction of anisotropy in western and eastern Iceland to be orthogonal to the ridge [34]. Our observations, however, show ridge-parallel fast directions in western Iceland at periods of 50–67 s, inconsistent with a simple passive flow model. We prefer the interpretation that weak azimuthal anisotropy at periods of 50–67 s in central Iceland is caused by the vertical alignment of olivine *a*-axes, suggesting a buoyant flow at depths greater than 50 km beneath the Icelandic rift zones. Buoyant flow has also been inferred beneath the Reykjanes Ridge above  $\sim 100$  km based on an inversion of Rayleigh and Love wave dispersions [19]. In contrast, at the fast-spreading East Pacific Rise, both shear-wave splitting results and Rayleigh wave data [24,28] show that fast directions are orthogonal to the ridge axis and argue for a passive, plate-driven mantle flow model. The active, buoyant flow beneath Iceland must be induced by hot thermal anomaly associated with the ridge-centered Iceland plume.

#### 4.4. Anisotropy constraints on ridge-parallel mantle flow

A striking feature of our Rayleigh wave inversions is the NNE–SSW, ridge-parallel anisotropic fabric beneath the rift zones in central Iceland at periods of 25–40 s and beneath western Iceland at 50–67 s (Fig. 9a,b). This ridge-parallel fast direction is consistent with seismic anisotropy in the crust in southwest Iceland obtained from shear-wave splitting [18]. Rayleigh waves at these periods are primarily sensitive to structure in the lower crust and uppermost mantle. One possible source of this anisotropy in the rift zones is fissuring and faulting in the crust. We have determined the magnitude of this possible crustal contribution by calculating the azimuthal anisotropy of Rayleigh waves propagating through models that have a 10 km thick layer with cracks aligned parallel to the ridge axis. Four different crack models from Shearer and Chapman [35] were used. The model with ‘thin dry cracks’ yields the strongest anisotropy, estimated at 1.8% at 25 s and 1.1% at

40 s. The decrease in crustal anisotropy with increasing period calculated from these models is not consistent with the relatively constant anisotropy observed for 25–40 s period Rayleigh waves (Fig. 9b). In addition, the strongest synthetic anisotropy is only half the size of the observed value at 40 s. We therefore conclude that while crustal fissuring may contribute to the observed anisotropy at periods less than 40 s, it cannot be the major source of anisotropy at longer periods. The most likely source of this anisotropy is in the underlying mantle.

A possible explanation of the ridge-parallel fast directions at 25–40 s beneath Icelandic rift zones is the systematic alignment of melt films which tends to orientate perpendicular to the least compressive stress [36–40]. The melting region beneath Iceland extends down to  $\sim 100$  km depth [6,7]. However, the preferred orientation of melt films cannot explain the weak anisotropy at periods of 50–67 s beneath the rift zones, corresponding to depths of 50–100 km. This would require that melt films preferably form above 50 km depth in the melting region, but this has not been clearly addressed in laboratory experiments and numerical models.

The most plausible explanation for the anisotropy observed beneath central and western Iceland is that it arises from the orientation of olivine fabric in the uppermost mantle. In this case, the ridge-parallel fast directions indicate mantle flow is preferentially channeled along the ridge axis above 50 km depth beneath the Icelandic rift zones and at depths of 50–100 km beneath western Iceland. The different depth of this channeling flow in central and western Iceland is probably due to the slope of oceanic lithosphere as it cools and thickens with age. Combined with the weak anisotropy observed at 50–67 s periods in the rift zones, the pattern of upper mantle anisotropy observed in central and western Iceland can be well explained by a simple model of buoyant upwelling at greater depths below 50 km and channeling of mantle flow at the base of the lithosphere beneath Iceland at shallower depths. The buoyant upwelling is presumably fed by the large amount of discharge from the Iceland plume and must be vigorous. When upwelling flow reaches

the base of the lithosphere, the slow spreading rate of the Mid-Atlantic Ridge and comparatively thick lithosphere beneath Iceland prevent the buoyant material from rising directly to the surface. The flow must change to a sub-horizontal direction at these depths. The slope of the lithospheric plates and the relatively low viscosity under the ridge axes form a natural channel for the material to flow along. Although the vertically aligned melt films in the mantle may contribute to the observed ridge-parallel anisotropy, the channeling of mantle flow along the ridge axes is likely the primary contribution to the observed ridge-parallel fast directions observed above 50 km beneath the Icelandic rift zones.

## 5. Conclusions

Our results suggest that the proximity of the Mid-Atlantic Ridge strongly influences the pattern of mantle flow associated with the Iceland plume. The buoyant flow associated with the Iceland plume arises from at least 100 km depth beneath Icelandic rift zones and the flow is significantly channeled along the Mid-Atlantic Ridge at the base of the lithosphere. We do not observe anisotropy that might be associated with radial flow away from the plume center in Iceland. Radial flow, if it exists, must be very weak, or in a small area close to the plume stem, or at depths greater than 100 km, which could not be resolved in our inversions. While plume–ridge interaction dominates mantle flow at shallow depths, it seems likely that asthenospheric flow in a generally N–S direction at depths greater than 100 km makes the dominant contribution to shear-wave splitting results observed in western Iceland. Iceland is thus a region of complex flow in the upper mantle, with variations in the pattern of flow both laterally beneath Iceland and with depth.

## Acknowledgements

We thank Yang Shen for providing data for the ICEMELT experiment and Karen Fischer for her constructive comments. Comments from three

anonymous reviewers were very helpful to improve this paper. This project is supported by a postdoctoral fellowship from the Woods Hole Oceanographic Institution to A.L. and NSF Grant OCE-0117938. **[SK]**

## References

- [1] P.R. Vogt, Asthenosphere motion recorded by the ocean floor south of Iceland, *Earth Planet. Sci. Lett.* 13 (1971) 153–160.
- [2] P.R. Vogt, Plumes, subaxial pipe flow, and topography along the mid-oceanic ridge, *Earth Planet. Sci. Lett.* 29 (1976) 309–325.
- [3] J.-G. Schilling, Iceland mantle plume geochemical evidence along Reykjanes ridge, *Nature* 242 (1973) 565–571.
- [4] M.A. Feighner, M.A. Richards, The fluid dynamics of plume-ridge and plume-plate interactions: An experimental investigation, *Earth Planet. Sci. Lett.* 129 (1995) 171–182.
- [5] N.M. Ribe, U.R. Christensen, J. TheiBing, The dynamics of plume-ridge interaction, 1: ridge-centered plumes, *Earth Planet. Sci. Lett.* 134 (1995) 155–168.
- [6] G. Ito, J. Lin, C.W. Gable, Dynamics of mantle flow and melting at a ridge-centered hotspot: Iceland and the Mid-Atlantic Ridge, *Earth Planet. Sci. Lett.* 144 (1996) 53–74.
- [7] G. Ito, Y. Shen, G. Hirth, C.J. Wolfe, Mantle flow, melting, and dehydration of the Iceland mantle plume, *Earth Planet. Sci. Lett.* 165 (1999) 81–96.
- [8] G. Ito, Reykjanes ‘V’-shaped ridges originating from a pulsing and dehydrating mantle plume, *Nature* 411 (2001) 681–684.
- [9] M. Albers, U.R. Christensen, Channeling of plume flow beneath mid-ocean ridges, *Earth Planet. Sci. Lett.* 187 (2001) 207–220.
- [10] I.T. Bjarnason, C.J. Wolfe, S.C. Solomon, G. Gudmundson, Initial results from the ICEMELT experiment: Body-wave delay times and shear-wave splitting across Iceland, *Geophys. Res. Lett.* 23 (1996) 459–462.
- [11] R.M. Allen et al., The thin hot plume beneath Iceland, *Geophys. J. Int.* 137 (1999) 51–63.
- [12] C.J. Wolfe, I.T. Bjarnason, J.C. VanDecar, S.C. Solomon, Seismic structure of the Iceland mantle plume, *Nature* 385 (1997) 245–247.
- [13] G.R. Foulger et al., Seismic tomography shows that upwelling beneath Iceland is confined to the upper mantle, *Geophys. J. Int.* 146 (2001) 504–530.
- [14] R.M. Allen et al., Imaging the mantle beneath Iceland using integrated seismological techniques, *J. Geophys. Res.* 107 (B12) (2002) 10.1029/2001JB000584.
- [15] Y. Shen, S.C. Solomon, I.T. Bjarnason, C.J. Wolfe, Seismic evidence for a lower-mantle origin of the Iceland plume, *Nature* 395 (1998) 62–65.
- [16] T. Tanimoto, D.L. Anderson, Mapping convection in the mantle, *Geophys. Res. Lett.* 11 (1984) 287–290.

- [17] A.E. Gripp, R.G. Gordon, Current plate velocities relative to the hotspots incorporating the NUVEL-1 global plate motion model, *Geophys. Res. Lett.* 17 (1990) 1109–1112.
- [18] W. Menke, B. Brandsdottir, S. Jakobsdottir, R. Stefansson, Seismic anisotropy in the crust at the mid-Atlantic plate boundary in south-west Iceland, *Geophys. J. Int.* 119 (1994) 783–790.
- [19] J.B. Gaherty, Seismic evidence for hotspot-induced buoyant flow beneath the Reykjanes ridge, *Science* 293 (2001) 1645–1647.
- [20] J.-P. Montagner, T. Tanimoto, Global anisotropy in the upper mantle inferred from the regionalization of phase velocities, *J. Geophys. Res.* 95 (1990) 4797–4819.
- [21] I.T. Bjarnason, P.G. Silver, G. Rumpker, S. Solomon, Shear wave splitting across the Iceland hotspot: Results from the ICEMELT experiment, *J. Geophys. Res.* 107 (B12) (2002) 10.1029/2001JB000916.
- [22] P.G. Silver, W.W. Chan, Shear-wave splitting and subcontinental mantle deformation, *J. Geophys. Res.* 96 (1991) 16429–16454.
- [23] C.J. Wolfe, P.G. Silver, Seismic anisotropy of oceanic upper mantle: Shear wave splitting methodologies and observations, *J. Geophys. Res.* 103 (1998) 749–771.
- [24] C.J. Wolfe, S.C. Solomon, Shear-wave splitting and implications for mantle-flow beneath the MELT region of the East Pacific Rise, *Science* 280 (1998) 1230–1232.
- [25] X. Yang, K.M. Fischer, Constraints on North Atlantic upper mantle anisotropy from S and SS phases, *Geophys. Res. Lett.* 21 (1994) 309–312.
- [26] B.H. Hager, R.J. O'Connell, Kinematic models of large-scale flow in the earth's mantle, *J. Geophys. Res.* 84 (1979) 1031–1048.
- [27] M.L. Smith, F.A. Dahlen, The azimuthal dependence of Love and Rayleigh wave propagation in a slightly anisotropic medium, *J. Geophys. Res.* 78 (1973) 3321–3333.
- [28] D.W. Forsyth, S. Webb, L. Dorman, Y. Shen, Phase velocities of Rayleigh waves in the MELT experiment on the East Pacific Rise, *Science* 280 (1998) 1235–1238.
- [29] A. Li, D.W. Forsyth, K.M. Fischer, Shear velocity structure and azimuthal anisotropy beneath eastern North America from Rayleigh wave inversion, *J. Geophys. Res.* 108 (2003) 2002JB002259, in press.
- [30] C.E. Nishimura, D.W. Forsyth, Rayleigh wave phase velocities in the Pacific with implications for azimuthal anisotropy and lateral heterogeneities, *Geophys. J.* 94 (1988) 479–501.
- [31] R.M. Allen et al., Plume-driven plumbing and crustal formation in Iceland, *J. Geophys. Res.* 107 (B8) (2002) 10.1029/2001JB000584.
- [32] F.A. Darbyshire, R.S. White, K.F. Priestley, Structure of the crust and uppermost mantle of Iceland from a combined seismic and gravity study, *Earth Planet. Sci. Lett.* 181 (2000) 409–428.
- [33] Y. Shen et al., Seismic evidence for a tilted mantle plume and north-south mantle flow beneath Iceland, *Earth Planet. Sci. Lett.* 197 (2002) 261–272.
- [34] D.K. Blackman et al., Teleseismic imaging of subaxial flow at mid-ocean ridges: traveltime effects of anisotropic mineral texture in the mantle, *Geophys. J. Int.* 127 (1996) 415–426.
- [35] P.M. Shearer, C.H. Chapman, Ray tracing in azimuthally anisotropic media: I. Results for models of aligned cracks in the upper crust, *Geophys. J.* 96 (1989) 51–64.
- [36] M.E. Zimmerman, S. Zhang, D.L. Kohlstedt, S.-I. Karato, Melt distribution in mantle rocks deformed in shear, *Geophys. Res. Lett.* 26 (1999) 1505–1508.
- [37] D.J. Stevenson, Spontaneous small-scale melt segregation in partial melts undergoing deformation, *Geophys. Res. Lett.* 16 (1989) 1067–1070.
- [38] J.-M. Kendall, Teleseismic arrivals at a mid-ocean ridge: effects of mantle melt and anisotropy, *Geophys. Res. Lett.* 21 (1994) 301–304.
- [39] U.H. Faul, D.R. Toomey, H.S. Waff, Intergranular basaltic melt is distributed in thin, elongated inclusions, *Geophys. Res. Lett.* 21 (1994) 29–32.
- [40] C.N. Richardson, Melt flow in a variable viscosity matrix, *Geophys. Res. Lett.* 25 (1998) 1099–1102.